J|A|C|S
ARTICLES
Published on Web 02/19/2005

Intramolecular Electron Transfer in Bis(methylene) Adamantyl Radical Cation: A Case Study of Diabatic Trapping

Lluís Blancafort,[†,*] Patricia Hunt,[‡] and Michael A. Robb[‡,*]

Contribution from the Institut de Química Computacional and Departament de Química, Universitat de Girona, E-17071 Girona, Spain, and Department of Chemistry, Imperial College London, South Kensington Campus, London SW7 2AZ, UK

Received October 7, 2004; E-mail: lluis.blancafort@udg.es; mike.robb@imperial.ac.uk

Abstract: Our characterization of the potential energy surface for electron transfer (ET) in the bis(methylene)-adamantane (BMA) model radical cation shows that the surface topology is prone to diabatic trapping (competition between ET and upward hops to the excited state). The general conditions for this phenomenon have been derived. The surface is centered around a conical intersection, and diabatic trapping occurs because one of the branching space coordinates (coordinates that lift the degeneracy at first order) corresponds to a vector of small length. For BMA, this coordinate is an antisymmetric breathing mode of the rigid carbon framework. Other modes (including methylene torsions and pyramidalizations) may lift the degeneracy at second-order but do not affect the energy gap at the intersection region effectively. The resulting topology is similar to that of an $(n - 1)$ dimensional seam (where n is the number of nuclear degrees of freedom of the molecule) that cannot be avoided along the reaction coordinate, thus favoring recrossing to the upper surface. This analysis is extended by ab initio semiclassical dynamics using an Ehrenfest and a trajectory surface hopping algorithm implemented at the CASSCF level. Examination of the trajectories shows that there is no single mode that controls the diabatic trap, in agreement with the condition that there is no predominant degeneracy-lifting coordinate. Thus the reactivity depends on a combination of small effects, where presumably higher-order effects come into play. This should be the general behavior of dynamics at a diabatic trapping situation.

Introduction

Recent ab initio calculations have demonstrated the role of avoided and real crossings (conical intersections) for intramolecular, ground-state electron transfer (ET) in several organic radical cations.[1−3] The crossing states are related to the states used in a Marcus treatment of ET, where the charge is localized on the donor, the acceptor, or the bridge of the ET system.[4−8] Ab initio calculations provide mechanistic information about the structural factors that govern the ET that cannot be obtained from a Marcus−Hush treatment. In several cases the calculated transition state on the potential energy surface was virtually coincident with a conical intersection (CI) between the ground and the excited state, strongly suggesting that the ET was affected by diabatic trapping. In diabatic trapping (or nonadiabatic recrossing), the reaction path from reactant to product passes through a region of the energy surface where the gap between the lower and the upper state is small enough to allow for population of the upper surface (Figure 1, where the region of interest is marked with a gray shadow). This slows down the reaction. An example is the photodissociation of bromoacetyl chloride and bromopropionyl chloride, where it is postulated that the overall reactivity does not depend on the relative size of the barrier along two competing channels but on nonadiabatic recrossing.[9−12] Diabatic trapping has also been postulated to be important in the wavelength-dependent photochemistry of the photoactive yellow protein chromophore.[13] Finally, it has also been observed in simulations of the reaction of lithium[14] and alumina[15] atoms with hydrogen.

Here we study the model bis(methylene) adamantane radical cation (BMA), where there is an intramolecular ET between two π bonds connected by the rigid adamantane framework (Scheme 1). BMA has been the subject of a mechanistic dynamics study by the groups of Carpenter and Paddon−Row,[16] using a semiempirical TSH method, which has partly motivated

[†] Universitat de Girona.
[‡] Imperial College London.

(1) Blancafort, L.; Adam, W.; González, D.; Olivucci, M.; Vreven, T.; Robb, M. A. *J. Am. Chem. Soc.* **1999**, *121*, 10583−10590.
(2) Fernández, E.; Blancafort, L.; Olivucci, M.; Robb, M. A. *J. Am. Chem. Soc.* **2000**, *122*, 7528−7533.
(3) Blancafort, L.; Jolibois, F.; Olivucci, M.; Robb, M. A. *J. Am. Chem. Soc.* **2001**, *123*, 722−732.
(4) Marcus, R. A. *Annu. Rev. Phys. Chem.* **1964**, *15*, 155.
(5) Sutin, N. *Prog. Inorg. Chem.* **1983**, *30*, 441−498.
(6) Newton, M. D. *Chem. Rev.* **1991**, *91*, 767−792.
(7) Paddon-Row, M. N. *Acc. Chem. Res.* **1994**, *27*, 18−25.
(8) Barbara, P. F.; Meyer, T. J.; Ratner, M. A. *J. Phys. Chem.* **1996**, *100*, 13148−13168.
(9) Lasorne, B.; Bacchus-Montabonel, M. C.; Vaeck, N.; Desouter-Lecomte, M. *J. Chem. Phys.* **2004**, *120*, 1271−1278.
(10) Bacchus-Montabonel, M. C.; Vaeck, N.; Lasorne, B.; Desouter-Lecomte, M. *Chem. Phys. Lett.* **2003**, *374*, 307−313.
(11) Butler, L. J. *Annu. Rev. Phys. Chem.* **1998**, *49*, 125−171.
(12) Forde, N. R.; Myers, T. L.; Butler, L. J. *Faraday Discuss.* **1997**, 221−242.
(13) Ko, C.; Levine, B.; Toniolo, A.; Manohar, L.; Olsen, S.; Werner, H. J.; Martinez, T. J. *J. Am. Chem. Soc.* **2003**, *125*, 12710−12711.
(14) Martinez, T. J. *Chem. Phys. Lett.* **1997**, *272*, 139−147.
(15) Chaban, G.; Gordon, M. S.; Yarkony, D. R. *J. Phys. Chem. A* **1997**, *101*, 7953−7959.

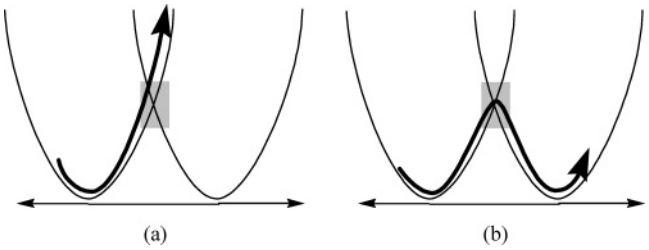

Figure 1. One-dimensional profile for nonadiabatic, ground-state ET (seam region marked in gray). (a) Surface hop. (b) "Direct" (quasi-adiabatic) ET.

Scheme 1

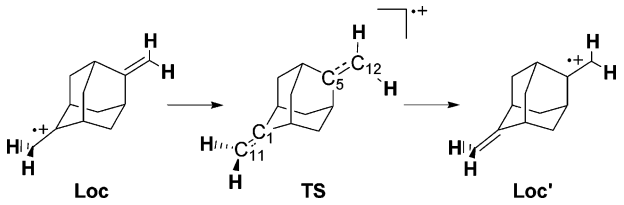

the present work. In this molecule, diabatic trapping occurs along the ground-state ET path. In the semiclassical picture that is the basis of our study, diabatic trapping appears as the alternative between "direct" (quasi-adiabatic) ET and hops to the excited state (Figure 1). The present work aims to identify the structural factors that affect this alternative in BMA and to establish the general conditions for diabatic trapping to occur on a potential energy surface. For this purpose we have used a potential energy surface analysis at the CI and CASSCF "on-the-fly" dynamics. Dynamics calculations are required to evaluate the alternative between surface hops and ET, and we have implemented two different algorithms for the treatment of nonadiabatic events in our CASSCF dynamic code, a trajectory surface hopping (TSH) algorithm[17,18] and Ehrenfest dynamics.[19,20] Predicting the reaction rate from the present dynamics calculations would require running a statistically significant number of trajectories at an accurate level of theory, which is not possible for the system studied here. However, we have used the dynamics results to obtain mechanistic information by inspecting the geometries for all the trajectories in the point of near degeneracy.

The nonadiabaticity for the ET in BMA can be predicted from symmetry arguments (there is zero super-exchange coupling, and the molecule is a Jahn−Teller system of D_{2d} symmetry). However, experimental results[21] show that BMA acts as an efficient bridge in intramolecular excited-state ET despite the nominal zero coupling. Carpenter[16] found that the torsion of the terminal methylenes plays a key role in the ET process, since it modulates the energy gap between the ground and the excited states, together with the π bond stretchings. This is in contrast to our later potential energy surface analysis,[3] where we found that the coordinate that controls the energy gap at the CI or transition state region, apart from the π bond sretchings, is an "antisymmetric breathing" of the rigid adamantane frame (Figure 2). However the effect of this coordinate on the energy gap is small, and the analysis of our calculated trajectories shows that there is no single mode that controls the alternative between ET and hop. On the contrary, the reactivity of the semiclassical trajectories in the region of the CI depends on a combination of small effects.

As we explain in more detail below, the general condition for diabatic trapping can be understood as follows. The approach to the crossing region takes place along one of the two coordinates that lift the degeneracy at the intersection to first-order (i.e., one of the branching space coordinates).[22−25] In BMA, this coordinate is the antisymmetric stretching of the two π bonds (gradient difference). A semiclassical trajectory will cross to the upper surface if it encounters the seam of intersection, but it will stay on the lower surface if it finds a way around the intersection through a region where the two surfaces are sufficiently separated. The coordinate that causes the splitting of the surfaces near the intersection region is the second branching space coordinate. The length of the corresponding vector determines the energy splitting induced by displacements along the coordinate. If this vector has small length, the splitting of the surfaces will be small, and the surface topology will correspond to a seam of quasi-degeneracy where upward recrossing is possible. Moreover, the transition structure for the reaction will lie very close to the CI. *Therefore diabatic trapping will occur when the length of one of the branching space vectors is small.* Such is the case for the breathing vibration of the BMA skeleton (interstate coupling), shown in Figure 2. The remaining vibrational degrees of freedom may modify the position of the seam of intersection along the reaction coordinate, but they do not affect the energy gap at the quasi-seam (excluding higher-order effects).

Computational Details

Semiclassical Algorithm Theory and Implementation for CASSCF Dynamics. We have implemented two different algorithms for the nonadiabatic event in MCSCF "on-the-fly" dynamics; a TSH algorithm[17,18] and an Ehrenfest algorithm.[19,20] "On-the-fly" methods use the electronic gradient to drive nuclear motion.[26,27] The nuclei are propagated on an adiabatic potential energy surface until the energy gap between the ground and excited states is small. After this point the possibility of a nonadiabatic event must be considered. There are two main possibilities, a surface hop or evolution inside the region of strong coupling. In surface hopping methods a decision is made whether to remain on the current state or to switch to another surface and consequently use a different gradient to propagate the nuclear motion. This type of method is most appropriate when recrossing is not considered to be likely, and it has been used by us on previous CASSCF studies.[28−30] The alternative Ehrenfest method, implemented here, propagates the nuclei on a potential energy surface obtained using a wave function which is a solution of the time dependent Schödinger

(16) (a) Jones, G. A.; Carpenter, B. K.; Paddon-Row, M. N. *J. Am. Chem. Soc.* **1999**, *121*, 11171−11178. (b) Jones, G. A.; Paddon-Row, M. N.; Carpenter, B. K.; Piotrowiak, P. *J. Phys. Chem. A* **2002**, *106*, 5011−5021.
(17) Bjerre, A.; Nikitin, E. E. *Chem. Phys. Lett.* **1967**, *1*, 179−181.
(18) Tully, J. C.; Preston, R. K. *J. Chem. Phys.* **1971**, *55*, 562−572.
(19) Herman, M. F. *Annu. Rev. Phys. Chem.* **1994**, *45*, 83−111.
(20) Chapman, S. *Adv. Chem. Phys.* **1992**, *82*, 423−483.
(21) DeCola, L.; Balzani, V.; Barigelletti, F.; Flamigni, L.; Belser, P.; Bernhard, S. *Recl. Trav. Chim. Pays-Bas* **1995**, *114*, 534−541.
(22) Migani, A.; Olivucci, M. In *Conical Intersections*; Domcke, W., Yarkony, D. R.; Köppel, H., Eds.; World Scientific: Singapore, 2004; Vol. 15, pp 271−320.
(23) Klessinger, M. M., Jr. *Excited States and Photochemistry of Organic Molecules*; VCH: New York, 1995.
(24) Bernardi, F.; Olivucci, M.; Robb, M. A. *Chem. Soc. Rev.* **1996**, *25*, 321−328.
(25) Yarkony, D. R. *J. Phys. Chem. A* **2001**, *105*, 6277−6293.
(26) Chen, W.; Hase, W. L.; Schlegel, H. B. *Chem. Phys. Lett.* **1994**, *228*, 436−442.
(27) Helgaker, T.; Uggerud, E.; Jensen, H. J. A. *Chem. Phys. Lett.* **1990**, *173*, 145−150.
(28) Worth, G. A.; Hunt, P.; Robb, M. A. *J. Phys. Chem. A* **2003**, *107*, 621−631.
(29) Boggio-Pasqua, M.; Ravaglia, M.; Bearpark, M. J.; Garavelli, M.; Robb, M. A. *J. Phys. Chem. A* **2003**, *107*, 11139−11152.
(30) Sánchez-Gálvez, A.; Hunt, P.; Robb, M. A.; Olivucci, M.; Vreven, T.; Schlegel, H. B. *J. Am. Chem. Soc.* **2000**, *122*, 2911−2924.

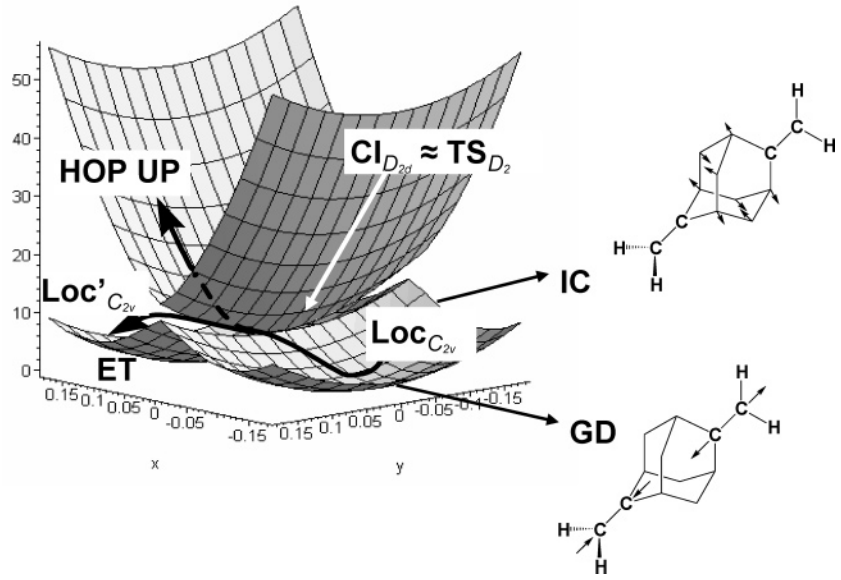

Figure 2. Two-dimensional plot of the potential-energy surface for nonadiabatic, ground-state ET in BMA in the seam region (projection along the gradient difference, GD, and interstate coupling, IC, coordinates). Reaction paths marked by arrows. Units: Displacement in au (*x*- and *y*-axes) and energy in kcal mol^{-1} (*z*-axis).

equation. This wave function is a linear combination of the adiabatic states, and because of this, the electronic wave function and thus the potential energy surface change continuously throughout the nonadiabatic event. The potential energy surface will eventually become one or other of the pure adiabatic states. Ehrenfest methods are particularly useful when the system remains for some time in the vicinity of a conical intersection, i.e., where it would otherwise make multiple crossings. Early implementations of this approach appear in the work of Delos and co-workers,[31] Billing,[32] and Gadea and co-workers.[33] More recently it has been successfully implemented within a molecular mechanics valence bond framework.[34] In addition to that, several improvements for both approaches have been proposed (for recent examples, see refs 35 and 36). Alternative treatments exist for introducing quantum mechanics into regions of nonadiabaticity; of particular note is the "multiple spawning" method of Martinez which spawns a new (nuclear) wave packet every time a region of strong interaction is encountered.[37,38] A frozen Gaussian is associated with each spawning, which is used to determine the population transfer. Details of all these methods can be found in a recent review.[39] The derivation of a time-dependent CASSCF wave function and the implementation of the hopping and Ehrenfest algorithms are given in the Supporting Information.

Potential Energy Surface for BMA and Calibration of SA-CASSCF(3,4)/STO-3G Level. In our dynamics calculations we use the SA-CASSCF(3,4)/STO-3G level of theory (active space of 4 π orbitals; SA = state-average). State-averaged orbitals over two states (with equal weights) are used to avoid discontinuities in the surface due to symmetry breaking. The use of a small basis set is imposed by the limitations of our computational resources (the dynamics require the solution of the SA-CP-MCSCF equations with 78 degrees of freedom, at every time step of the trajectory). The quality of the basis set is calibrated against SA-CASSCF(3,4)/6-31G*//SA-CASSCF(3,4)/3-21G* values (optimization of the critical points at the SA-CASSCF-(3,4)/3-21G* level and recalculation of the energetics at SA-CASSCF-(3,4)/6-31G*). Relative energetics and the most relevant structural parameters at both levels of theory are compared in Table 1. For our dynamics calculations, the most relevant point is the reduction of the energy gap at the D_2 "transition structure" (**TS**) from 0.47 kcal mol^{-1} to 0.23 kcal mol^{-1} with the STO-3G basis. This means that the dynamics calculations overestimate the tendency for a surface hop. The potential energy surface used for the dynamics shows other limitations due to the level of calculation. The D_2 symmetry structure appears as a true minimum because no imaginary frequencies were obtained at both levels of theory.[3] However, no transition structure could be located between the D_2 and the C_{2v} structures, and a linear interpolation showed a monotonic energy decrease between the two. This indicates that the D_2 structure is a very shallow minimum that can be taken as the ET transition structure, **TS**. The localized C_{2v} structure **Loc** is a true minimum with the STO-3G basis set, but it has a small imaginary frequency (135i cm^{-1}) with the 3-21G* basis, although no minimum of lower symmetry could be found with this basis. As we discussed in our previous study of the potential energy surface of BMA,[3] the semiempirical method used in the study of Carpenter and co-workers[16] gives a different structure for the minimum **Loc**, where the C_{2v} symmetry was lost because the charge-bearing methylene was twisted

Table 1. Energetics and Structural Parameters for the Critical Points of BMA at the SA-CASSCF(3,4)/6-31G*//SA-CASSCF(3,4)/3-21G* and SA-CASSCF(3,4)/STO-3G Levels of Theory

structure		STO-3G	6-31G*//3-21G*
Loc (C_{2v})	E_{rel} [kcal mol^{-1}]	0.0	0.0
	r_{C1-C11}/r_{C5-C12} [Å]	1.440/1.343	1.419/1.337
	ν_{C1-C11} [cm^{-1}]^a	1743 (2.49)^b	1603 (2.29)^b
	ν_{C5-C12} [cm^{-1}]^a	1918 (2.74)^b	1810 (2.59)^b
TS (D_2)	E_{rel} [kcal mol^{-1}]	4.57	3.30
	ΔE [kcal mol^{-1}]^c	0.23	0.47
	r_{C1-C11}/r_{C5-C12} [Å]	1.389	1.375
CI (D_{2d})	E_{rel} [kcal mol^{-1}]	4.52	3.24
	r_{C1-C11}/r_{C5-C12} [Å]	1.389	1.375

^{a} Frequency of the corresponding carbon−carbon stretch. ^{b} Zero-point energy [kcal mol^{-1}] in brackets. ^{c} Energy gap between ground and excited state.

(31) Delos, J. B.; Thorson, W. R.; Knudson, S. K. *Phys. Rev. A* **1972**, *6*, 709−720.
(32) Billing, G. D. *Chem. Phys. Lett.* **1975**, *30*, 391−393.
(33) Amarouche, M.; Gadea, F. X.; Durup, J. *Chem. Phys.* **1989**, *130*, 145−157.
(34) Klein, S.; Bearpark, M. J.; Smith, B. R.; Robb, M. A.; Olivucci, M.; Bernardi, F. *Chem. Phys. Lett.* **1998**, *292*, 259−266.
(35) Jasper, A. W.; Stechmann, S. N.; Truhlar, D. G. *J. Chem. Phys.* **2002**, *116*, 5424−5431.
(36) Zhu, C. Y.; Jasper, A. W.; Truhlar, D. G. *J. Chem. Phys.* **2004**, *120*, 5543−5557.
(37) Ben-Nun, M.; Martinez, T. J. *J. Chem. Phys.* **1998**, *108*, 7244−7257.
(38) Martinez, T. J.; BenNun, M.; Levine, R. D. *J. Phys. Chem.* **1996**, *100*, 7884−7895.
(39) Worth, G. A.; Robb, M. A. In *Role of Degenerate States in Chemistry*, 2002; Vol. 124, pp 355−431.

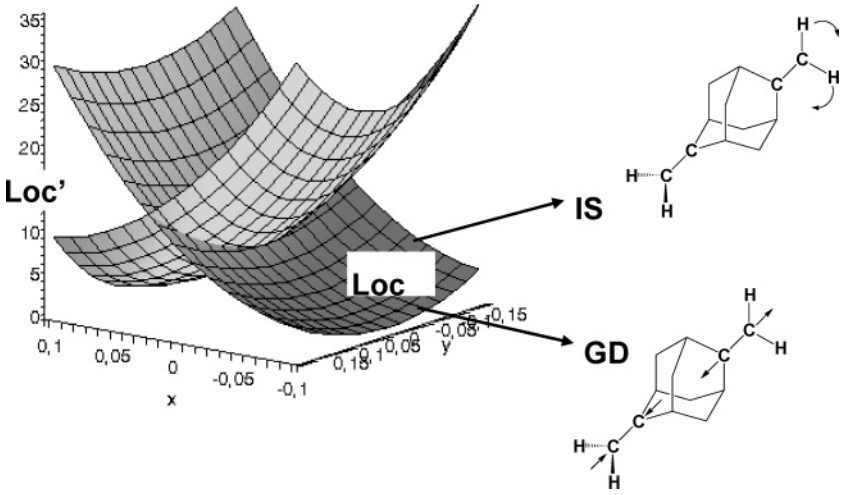

Figure 3. Two-dimensional plot of the potential energy surface for BMA (seam of intersection) projected along the GD and one methylene torsion intersection space mode (IS). Units: Displacement in au (*x*- and *y*-axes) and energy in kcal mol^{-1} (*z*-axis).

and pyramidalized. This is supported by results on the radical cation of ethylene.[16] Therefore the level of calculation used here cannot reproduce the details of the entire potential energy surface, but it provides a correct qualitative description in the region of near degeneracy. Thus our calculations allow us to draw valuable conclusions about the topology of the surface and the mechanism of the ET.

Second-Order Analysis at the Conical Intersection. We have analyzed the curvature of the surfaces of the two degenerate states at the conical intersection by calculating the Hessian for the two states. The Hessians are diagonalized in the space of the $n - 2$ intersection space (IS) modes (where n is the number of nuclear degrees of freedom of the molecule), after eliminating the two branching space coordinates by projection, together with the rotation and translation coordinates.[40] The results of this calculation (force constants and second-order splittings along the IS modes) are listed in the Supporting Information (Table SI1). Figure 3 shows the potential energy surface along the GD and one IS mode. The figure is based on a second-order Taylor expansion around the CI along the GD and IS modes, and it is valid for any of the $(n - 2)$ IS modes. It shows that the seam of intersection is a curve rather than a straight line parallel to the IS axis.[40] In the topology presented in Figure 3, displacements in a closed loop around the CI should encounter the intersection seam twice. We have carried out this proof for a methylene torsion where the curvature difference is approximately 0.025 au, by displacing the CI geometry along combined displacements of the two coordinates and calculating the energies of the two states. The results agree with the expansion-based plot of Figure 3; i.e., the seam lies along a curved line (combination of the GD and methylene torsion mode; see Supporting Information for details).

Trajectory Details and Initial Conditions. Our dynamics calculations are carried out using the "on-the-fly" methodology for classical and semiclassical dynamics implemented in Gaussian03[41] by Schlegel and co-workers.[26,27] The gradient and curvature of the surface are evaluated locally at every step of the trajectory, including a fifth-order correction of the potential energy surface. To study the ground-state intramolecular ET, trajectories were started at the localized minimum of C_{2v} symmetry, randomly sampling the zero-point energy of all 78 degrees of freedom. Under these conditions, the region of the seam is accessed on average after less than 100 fs, i.e., after approximately 200 steps. Thus, at the level of calculation used for the dynamics (SA-CASSCF(3,4)/STO-3G), the energy difference between the localized minimum and the D_2 transition structure is 4.52 kcal mol^{-1}. The frequencies for the two π bonds at the localized geometry are 1742.9 cm^{-1} for the singly occupied bond and 1917.9 cm^{-1} for the doubly occupied bond, which corresponds to zero-point energies of 2.49 and 2.74 kcal mol^{-1}, respectively. The reaction coordinate is the antisymmetric combination of the bond stretchings, and the region of the seam is low enough in energy that it can be reached if the two bonds oscillate with opposite phase, or after intramolecular vibrational energy redistribution from other modes into these bond stretchings.

After the sampling step, the trajectories were run in the ground state using an "adiabatic algorithm" (step size 0.25 sqrt(amu)*bohr, approximately 0.5 fs). The "semiclassical algorithm" was switched on at a threshold value of less than 8 mhartrees (4.8 kcal mol^{-1}) for the D_2-D_1 energy gap. Trajectories were first run using the TSH algorithm, adjusting the step size to 0.05 sqrt(amu)*bohr (approximately 0.1 fs). Surface hops were carried out when the ground-state probability of the time-dependent wave function went below a threshold value of 0.65. The stability of the results against this parameter was checked for a hexatriene test system, and changes of ± 0.2 in the threshold had little effect on the hop point. To avoid excessive multiple hopping, the minimum time between a hop and the next one was set to 1.0 fs. This value is small enough to treat the passage through the CI because the vibrational period of the antisymmetric stretching of the π bonds (which is the coordinate that drives the reaction through the seam region) is 1 order of magnitude higher (10−20 fs; see Chart 3). Changes in these two parameters can be important for trajectories which go through a "mixed state" (see the Results of Dynamics Calculations section below), but in these cases the Ehrenfest method is preferable.

Whenever hops or ET were detected with the TSH algorithm, the trajectories were rerun with the Ehrenfest algorithm, using the geometries and velocities before the event of interest as starting conditions. The step size for these runs was adjusted to 0.02 sqrt(amu)*bohr (approximately 0.04 fs). The exit threshold was 15 mhartrees (9.0 kcal mol^{-1}) for both algorithms.

Analysis of the Trajectories. Our study of the calculated trajectories focuses on the behavior of the molecule in the *region of the seam* (region of near degeneracy), where the alternative between ET and surface hop occurs. In this region of the potential energy surface, the energy gap between the two states is small, and there is a finite degree of mixing between the two states (i.e., ground-state probability of the time-dependent state differs from 1.0). At the same time, the π bonds become similar in length and the charge delocalizes. In our analysis, we consider the following parameters (see Charts 1−3): (1) Energy gap between the adiabatic states. (2) Probabilities for the state of interest, obtained by projection of the time-dependent state on the two adiabatic

(40) Paterson, M. J.; Bearpark, M. J.; Robb, M. A.; Blancafort, L. *J. Chem. Phys.* **2004**, *121*, 11562−11571.
(41) Frisch, M. J. et al. *Gaussian03*, revision B.02 ed.; Gaussian, Inc.: Pittsburgh, PA, 2003.

Chart 1. Energy Gap along a Trajectory with an Unreactive Surface Hop Pair (3−8 fs) and Quasi Adabatic ET (approximately 25 fs)

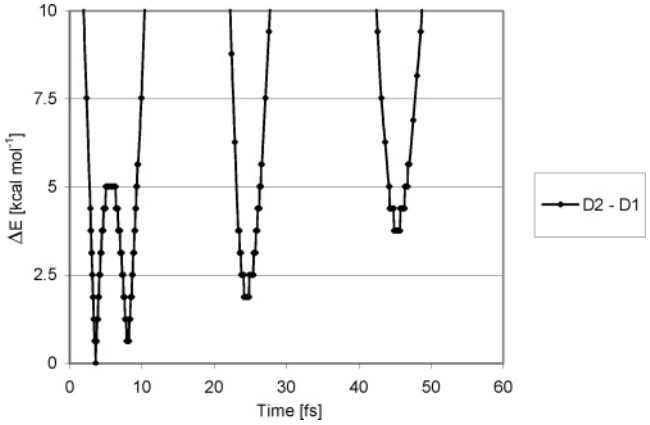

Chart 2. Probabilities for the Two States along a Trajectory with an Unreactive Surface Hop Pair (3−8 fs) and Quasi Adabatic ET (approximately 25 fs)

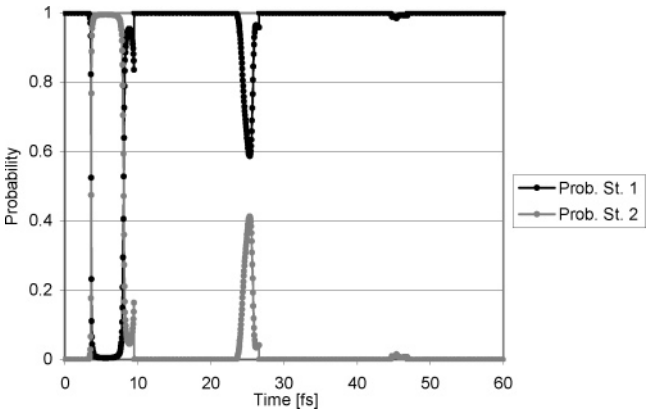

Chart 3. Length of the C_1-C_{11} and C_5-C_{12} Bonds along a Trajectory with an Unreactive Surface Hop Pair (3−8 fs) and Quasi Adabatic ET (approximately 25 fs)

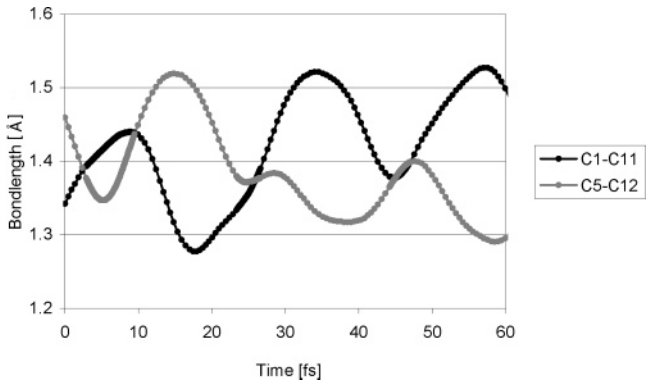

states. The probabilities are used to monitor the hops (switch from 1.0/0.0 for ground and excited state to 0.0/1.0). (3) Length of the π bonds (C_1-C_{11} and C_5-C_{12}, respectively; see Scheme 1 for atom numbering). On average, the bond where the charge is localized is longer, and the lengths of the π bonds are inverted during the surface hops and ET. Occurrence of ET was confirmed by examining the occupation of the π bonds for the adiabatic ground-state wave function (D_1 state) at the exit of the seam region. Using these parameters we have classified our trajectories in four different types: (a) unreactive hop pair, (b) direct ET, (c) reactive hop pair with ET in the excited state, and (d) extended mixed state. In the Results section we describe one example for cases (a) and (b). Case (c) is the reverse of case (b), and an example for case (d) is described in the Supporting Information.

Theoretical Analysis of the Potential Energy Surface Topology

In our preceding studies of ground-state intramolecular ET in organic radical cations, we showed for several cases that the surface topology is centered around a conical intersection (CI) between the ground and the excited state of the molecule (see Figure 2).[1−3] The ground-state topologies have the shape of a "moat" spanned by the two degeneracy-lifting coordinates at the intersection, the gradient difference ($GD = [\partial(E_1 - E_2)]/\partial Q]$), and the interstate coupling ($IC = \langle Y_1(\partial H/\partial Q)\Psi_2\rangle$). These coordinates form the branching space of the intersection, and the energy of the states remains degenerate (to first-order) along the remaining $n - 2$ vibrational modes, which form the intersection space. The relevant structures for ET (the minima **Loc** and **Loc′**, where the charge is localized in the donor or the acceptor, and the charge-delocalized transition structures or intermediates) lie in the "moat". **CI** is a point on an extended conical intersection line, which provides a locus for nonadiabatic population transfer to the excited state. The transition state for the reaction lies in the space orthogonal to this line as shown in Figure 2. Therefore direct ET must avoid or surround the intersection, going through the outer region of the cone. In several molecules studied previously, this is possible and there are adiabatic ET paths on the potential energy surface. However, in limiting cases where one of the two corresponding vectors GD or IC has a nearly zero length, the surface crossing becomes only weakly avoided because the energy gap created by displacement along this coordinate depends on the length of this vector. Therefore the topology becomes similar to that of an $(n - 1)$-dimensional seam of intersection, as in a singlet−triplet crossing.[2,3] At the same time, the minimum associated with displacement along the IC vector (the TS for ET in the present case) lies very close to the intersection. Thus, the resulting moat that surrounds the intersection contains a sharp ridge, and the upper part of the cone remains close to the lower surface. The minimum energy reaction path (bold arrow in Figure 2) passes very close to the conical intersection, and hops to the upper surface become possible. Similar situations, where one of the degeneracy lifting vectors is exactly zero, have been characterized by Yarkony and co-workers as confluences of intersection seams in tri- and tetratomic systems.[42]

In BMA, the relevant structures (Scheme 1) are the localized minimum of C_{2v} symmetry, where the charge is localized on one of the π bonds (**Loc** and **Loc′**); the delocalized minimum of D_2 symmetry, which functions as the ET transition structure (**TS**); and the Jahn−Teller degenerate species of D_{2d} symmetry, which was optimized as a conical intersection (**CI**). For this structure of D_{2d} symmetry, the degenerate orbitals form a localized basis. Therefore the modes of the branching space have b_1 and b_2 symmetry for the interstate coupling and the gradient difference, respectively, and displacement from the CI along these modes leads to structures **TS** and **Loc**/**Loc′**, respectively (see Figure 2). The gradient difference of b_2 symmetry is the antisymmetric π bond stretching and corresponds to the "intuitive" reaction path coordinate. Along this coordinate, the conical

(42) Matsika, S.; Yarkony, D. R. *J. Phys. Chem. A* **2002**, *106*, 2580−2591.

intersection has a peaked shape; i.e., the two minima lie on different sides of the intersection.[43] The interstate coupling of b_1 symmetry is an "antisymmetric breathing" of the adamantane framework. The degeneracy-lifting character of this coordinate can be understood in the context of the superexchange mechanism of electronic coupling.[7] According to this mechanism, the splitting between the electronic states in ET or similar processes arises from interaction of the donor and acceptor molecular orbitals. In the superexchange mechanism, this interaction occurs through the σ bonds of the bridge that connects the donor and the acceptor. In BMA, the overall superexchange interaction is canceled out at D_{2d} structures because of the symmetry of the bridge, but the symmetry breaking distortion of the σ orbital frame lifts the degeneracy. However, the length of the IC vector is small and the surface topology around the CI corresponds to the case described above.

To get a quantitative estimate of the probability of nonadiabatic behavior it is necessary to consider the length of the IC vector and the curvature of the surface along that coordinate. The estimate is based on a simple second-order expansion of the energy around the CI, where the two states are described as equivalent parabolas that cross at the CI. The approach is similar to the one used to relate energy barriers to reorganization energy in Marcus theory (see Supporting Information for details, section SI2.1).[8] The energy gap at a minimum along a first-order degeneracy-lifting coordinate x associated to a CI can thus be predicted from two parameters calculated at the CI, the gradient of the surfaces at the CI and the force constant along the coordinate ($g_{x,\mathrm{CI}}$ and k_x, respectively):

$$\Delta E_{\min} = \frac{2{g_{x,CI}}^2}{k_x} \qquad (1)$$

In the present case (CASSCF(3,4)/3-21G* data), the gradient of the surfaces at the CI is half the length of the IC vector (0.0064 au), whereas the force constant along the IC "antisymmetric breathing" mode is estimated as approximately 0.25 au from the calculated force constants for the remaining intersection-space modes (see below and entry 53 of Table SI1, Supporting Information). The calculated value of approximately 0.2 kcal mol^{-1} (0.009 eV) is the energy gap at the D_2 minimum along the IC coordinate (**TS**), estimated from the parameters calculated at the CI. This value is lower than the estimated limit of 0.025 eV for the adiabatic regime,[44] and the ET can be predicted to be nonadiabatic. Clearly the second-order based expansion has its limitations, and one should be careful when applying this approach to estimate the energy gap at a minimum associated to a CI. However, the actual energy gap at the optimized **TS** structure (at the CASSCF(3,4)/3-21G* level) of 0.13 kcal mol^{-1} (0.0054 eV) is close to the predicted value, which indicates that the approach is useful here, presumably because of the rigidity of the molecule.

To evaluate the effect of the remaining $n - 2$ vibrations (the intersection space, IS) on the energy gap at the region of conical intersection, we have carried out an analysis of the curvature of the two intersecting surfaces along these coordinates (see Computational Details).[40] The energy of the states remains degenerate along them to first order, but there can also be a second-order lifting of the degeneracy which is analogous to the Renner−Teller effect (Figure 4). Thus the surfaces of the two states can have different curvatures along the IS modes. In BMA, the modes with the most significant second-order degeneracy lifting effects (see Table SI1 and Figure SI2, Supporting Information) are methylene vibrations (for example torsion or pyramidalization) as well as vibrations of the adamantane framework. For the methylene torsions and pyramidalizations, for example, the curvature of the two states differs by approximately 0.050 and 0.023 au, respectively, whereas, for some skeletal deformations, the most significant differences are 0.012−0.082 au (to illustrate these figures, displacement along the methylene torsion mode by 1 au, which should induce an energy gap of approximately 0.050 au or 30 kcal mol^{-1}, corresponds to a torsion of 21°). These values have the same order of magnitude as the length of the IC vector, and it could be conceivable that they contributed to lifting of the degeneracy at the intersection, favoring the ET reactivity of BMA. To show that this is not the case we have plotted the energy along the GD and one IS mode in Figure 3, neglecting the effect of the IC mode. The calculated surface is qualitatively different from the one formed by the GD and IC modes (Figure 2). Thus the main effect of the "curvature difference" along the IS mode is *not* to eliminate the degeneracy but to turn the intersection seam from a straight line along the IS coordinate into a curve (see Computational Details). Therefore trajectories in the reduced GD/IS space would always find the seam on their way from reactant to products. When the full dimensionality of the system is considered, the "curvature difference" along any of the IS modes does not increase the energy gap along the IC coordinate (although it displaces the quasi-seam along a curved coordinate). From a mechanistic point of view, then, the energy splitting caused by the IS modes does not contribute to avoiding the diabatic trap. Thus the only coordinate that can lift the degeneracy (excluding higher-order effects) and effectively avoid the crossing is the IC.

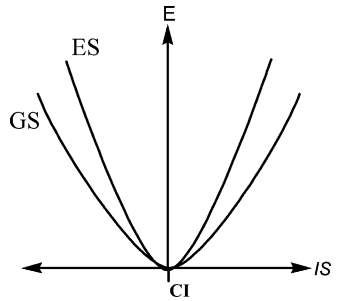

Figure 4. "Curvature difference" (Renner−Teller type profile) between the ground (GS) and the excited state (ES) at a CI caused by second-order splitting along an intersection space mode (IS).

Results of Dynamics Calculations

Summary. We ran 25 trajectories for an average of 130 fs per trajectory, with a total of 53 events in the region of the seam (including upward and downward hops; see Table SI2, Supporting Information). There were 5 cases of direct ground-state ET and 17 cases of upward surface hop, followed by a downward hop. In 13 of these cases, the hop pair was unreactive (= recrossing). In 3 cases, there was an excited-state ET before the downward hop, yielding a reactive hop pair. In the remaining case there were two excited-state ET events before the down-

(43) Atchity, G. J.; Xantheas, S. S.; Ruedenberg, K. *J. Chem. Phys.* **1991**, *95*, 1862−1876.
(44) Farazdel, A.; Dupuis, M.; Clementi, E.; Aviram, A. *J. Am. Chem. Soc.* **1990**, *112*, 4206−4214.

ward hop, yielding a net unreactive hop pair. This gives a total of 5 excited-state ET events. We also found three cases of an extended, unreactive mixed state (lasting approximately 2 fs). Finally, six ambiguous cases were discarded. The ratio between quasi-adiabatic ET and hops obtained here is of the same order of magnitude than the one found in the semiempirical study of the Carpenter and Paddon-Row groups.[16]

Unreactive Hop Pair and Direct ET. Charts 1−3 show the data for a trajectory during 60 fs (approximately 400 time steps). The trajectory contains one hop pair and one ET event. Initially there is a fast access to the seam region with an unreactive hop pair (hop up at 3.6 fs and hop down to 8.1 fs). At the hops, the energy gap between the states is close to zero (see Chart 1). Chart 2 (probabilities) gives the description of the D_1 state (ground state) in terms of the quasi-diabatic, charge localized states. At the hops, the probabilities (Chart 2) change quickly, indicating that the hops are quasi-diabatic (i.e., the charge remains localized on one bond, and there is no ET). Chart 3 also shows that at the moment of the hops the two π bonds have similar length. After the unreactive hop pair, the trajectory has another encounter with the region of the seam at approximately 25 fs, which results in a "direct", quasi-adiabatic ET. The energy gap during the ET remains larger than at the hops (approximately 2 kcal mol^{-1}), and the state can be described as a "mixed state" (see the probabilities in Chart 2). After the ET, the relative lengths of the π bonds (Chart 3) are inverted; i.e., the C_1-C_{11} bond becomes longer, and the C_5-C_{12}, shorter. This corresponds to charge transfer from C_5-C_{12} to C_1-C_{11}. On Charts 1−3 it can be also seen that around 45 fs there is a "frustrated" attempt to access the seam, where the bonds become equal in length but the energy gap is not small enough. This shows that factors other than the bond lengths have an effect on the energy gap and the reactivity.

Ambiguous Cases. Of the 56 calculated events, 9 gave ambiguous results with the Ehrenfest code. In three cases, changes in the orbital basis during the CASSCF calculations (orbital rotations caused by localization or delocalization) induced discontinuities in the energy and the probabilities of the time-dependent state, and the results were discarded. In six other cases, the orbital rotations caused unphysical "mixed states" (mix of the probabilities with an energy gap larger than 0.005 hartree or 3 kcal mol^{-1}). This problem is related to the typical Ehrenfest pathology, where the trajectory leaves the region of near degeneracy (increasing energy gap between ground and excited state) in an unphysical mixed state.[45] Two of these events were satisfactorily re-evaluated with the TSH algorithm. In one trajectory, the unphysical mixing occurred before accessing the region of near degeneracy and the trajectory was repeated successfully with a reduced entrance threshold to the time-dependent algorithm (0.005 hartree). The results of these trajectories are included in Table 1. The remaining three trajectories with unphysical mixed states were discarded, adding to a total of six.

Comparison of the Ehrenfest and TSH Algorithms. To compare the performance of the two methods, 18 trajectories were run using the two algorithms, under the same initial conditions at the threshold to the seam region. The results are then compared in terms of the net reactivity of the event and, on a more detailed level, the final conditions (geometry and velocities at the exit of the seam region). Overall, the comparison shows that the TSH method implemented here is reliable for the surface hops because they are quasi-diabatic. Thus, it yields the same final conditions as the Ehrenfest method in five out of six cases; in the remaining case, the net reactivity is predicted correctly (unreactive surface hop), but different final conditions are obtained. The divergence between the methods is more significant in the case of direct ET. Here the TSH method only reproduces the Ehrenfest exit conditions in two out of five cases. In two more cases, the reactivity (direct ET) is predicted correctly by the TSH method but with different exit conditions. In one more case the TSH method fails and predicts a surface hop where the Ehrenfest method gives direct ET through a short "mixed state". The results also diverge for the cases of extended "mixed state", where the TSH method gives a succession of hops and yields different final conditions. In contrast to this, two cases where the Ehrenfest algorithm fails because of unphysical mixed state were re-evaluated successfully with the TSH algorithm. Overall, the good agreement between the TSH and Ehrenfest methods for the quasi-diabatic hops indicates that the two methods are valid approximations for these cases. The bigger discrepancies found for the cases of direct ET are understandable because in those cases the charge has to delocalize at the same point of the trajectory. The use of a "mixed-state" potential is helpful to describe this charge delocalization, and therefore the Ehrenfest method should be better here. Clearly wave packet dynamics methods would be more reliable, but they seem difficult to apply here in view of the many degrees of freedom. For a comparison between the TSH and a wave packet method for the smaller butatriene radical cation, the reader is referred to ref 27.

Discussion

Our dynamics calculations show, in agreement with the earlier dynamics study of Carpenter and co-workers,[16] that diabatic trapping occurs in the ET of BMA. Therefore we have confirmed our proposal that the potential energy surface, centered around a conical intersection, is prone to diabatic trapping because one of the branching space vectors has almost zero length. In addition to that, our mechanistic analysis aims to validate the prediction given by our analysis of the conical intersection region, namely that the alternative between electron transfer and diabatic trapping at that region is not controlled by a single mode because the IC has vanishing length. For this purpose we have analyzed the "transition structures" of all the trajectory points with direct ET and the "hop structures" for all trajectories with a surface hop (Tables SI3−SI7, Supporting Information). Our general assumption is the usual Marcus model for ET[4] and the Landau−Zener treatment for avoided crossings,[6] where the probability of hops at points of near degeneracy on a potential energy surface depends mainly on the energy gap between the states of interest. Our results agree with this model, since the energy gap is bigger than 1 kcal mol^{-1} in all cases of direct ET, although we find some surface hops with energy differences up to 1.9 kcal mol^{-1}. In these cases, the surface hop is induced by a dynamic factor, the velocity of the trajectory when it reaches the seam, which is also in agreement with the Landau−Zener treatment.

Analysis of the structural parameters at the point of near degeneracy shows that there is no clear-cut correlation between these parameters and the reactivity. Thus, the average torsion

(45) Hack, M. D.; Truhlar, D. G. *J. Phys. Chem. A* **2000**, *104*, 7917−7926.

at the hops is 6.7°, and the one for ET is 6.9°. Moreover, only one ET trajectory goes through the seam with a torsion of more than 10°, and there are several cases of surface hops with bigger torsions. A similar lack of correlation between reactivity and structure in the region of the seam is found for the IC coordinate, the antisymmetric breathing skeletal mode. The value for this coordinate is evaluated by comparing the changes in the distances between the vibrating carbons (see Supporting Information), and we find average changes of 0.057 Å for the trajectories with surface hop and 0.066 Å for the ones with direct ET. Similar results are found for the methylene pyramidalization angles and the difference in length of the two relevant π bonds ($\Delta r_{(CC)}$ value in Tables SI3−SI7). This analysis strongly supports our view of the diabatic trap being controlled by a combination of vibrations with small effects rather than by a single mode.

In contrast to our conclusion, the preceding study by the Carpenter and Paddon−Row groups highlighted the role of the methylene torsion in modulating the energy gap for the ET.[16] This conclusion was based on a Fourier transform analysis of the energy gap during the whole trajectory, where one of the peaks in the spectrum is assigned to the methylene torsion. However, in our analysis of diabatic trapping we distinguish the factors that influence the approach to the conical intersection region from the ones that modulate the outcome of the trajectories. In fact the methylene torsion is important for the approach to the seam region, as it affects the energy difference *at charge-localized structures*. We have recognized this effect by carrying out finite displacements, starting from **Loc**, along the normal mode corresponding to the methylene torsion of the doubly occupied π bond (see Chart SI5, Supporting Information). The change of the energy gap along this coordinate is the origin of the effect observed in the result of the Fourier transformation.[16] However our argument is based on the fact that the energy gap induced by the methylene torsion *at the intersection region* has its origin in the curvature difference (a second-order effect) at the CI. As we have discussed above with the help of Figure 3, the surface splitting caused by this mode does not increase the energy gap effectively. On the contrary, avoiding the crossing requires a significant displacement along the IC coordinate.

Conclusions

The ET reaction in the model radical cation BMA is prone to diabatic trapping because the surface topology is centered around a conical intersection which is virtually coincident with the transition structure for the reaction. The occurrence of diabatic trapping can be rationalized by an analysis of the relevant coordinates at the conical intersection. Thus the approach from the reactant to the seam region is regulated by one of the branching space coordinates that lift the degeneracy at first-order. The other degeneracy lifting coordinate controls the gap between the lower and upper states at the seam region. It facilitates the avoided crossing path for ET that surrounds the CI. In the BMA case, the corresponding vector has almost zero length. As a consequence, the ET transition structure is virtually coincident with the CI, and the crossing cannot be avoided. The remaining $(n - 2)$ coordinates may lift the degeneracy at second-order, but they do not effectively increase the energy gap at the intersection region. Thus the topology can be described as an $(n - 1)$-dimensional seam of intersection.

Our characterization of the topology as prone to diabatic trapping is confirmed by semiclassical ab initio CASSCF dynamics with an Ehrenfest and a trajectory surface hopping algorithm. Examination of the trajectories at the structures where the alternative between ET and recrossing is decided shows that there is no single vibrational coordinate that determines the reactivity. None of these coordinates has a dominating effect, and the reactivity appears to be the result of many small effects. Presumably effects of a higher-order that have not been considered in our analysis are important in this case.

The topology plotted in Figure 2 for the intramolecular ET in BMA is similar to the one described in the work of Butler and co-workers for the photochemical dissociation of bromoacetyl and bromopropionyl chlorides, based on experimental and theoretical results.[11,12] As emphasized by these authors, the origin of the recrossing does not lie in the fact that the reaction is "symmetry forbidden". In fact, it becomes "symmetry allowed" when the molecule loses its symmetry. However, the reason for nonadiabaticity is that the reaction transition structure is close to a conical intersection. The same explanation can be given for our BMA ground-to-excited-state recrossing. Thus, at D_{2d} geometries, the ET is "symmetry forbidden" and there is zero super-exchange coupling between the two π bonds. At D_2 geometries, the ET becomes "symmetry allowed". However, nonadiabaticity appears because the vector that displaces the geometry from the CI to the transition structure is small. In fact the preceding explanation for bromoacetyl chloride has been recently put to doubt by Fang and co-workers,[46] who found no evidence of a state crossing in the vicinity of the dissociation transition structure. Nevertheless, the general model described by Butler remains valid, as our results show, regardless of whether it may apply to the bromoacetyl chloride case or not. A similar topology, where a TS lies close to a CI between two excited cases, has also been given as the explanation for diabatic trapping in the photoinduced isomerization of the photoactive yellow protein chromophore.[13]

The similarity between the BMA case and the cases described above shows that the conditions given here for diabatic trapping must be quite general. They can be understood in terms of the two branching space coordinates. Diabatic trapping can be expected in cases where the reaction path passes through a conical intersection region or near to it (i.e., when the reaction coordinate is one of the branching space coordinates) and when the vector corresponding to the other branching space coordinate has small length. In the context of similar dynamics studies,[47] it has been proposed that diabatic trapping or recrossing would be favored by a sloped or tilted topology[43] of the conical intersection, because at peaked topologies the trajectories are moved away from the intersection. However the present study shows that diabatic trapping is possible in peaked topologies, and therefore we conclude that the determining factor is the nearly zero length of one branching space vector. The small length of this vector is also the origin of the dynamic behavior, where there is no mode that regulates the behavior at the diabatic trap preferentially. We expect this to be a general characteristic of diabatic trapping for cases as the present one, where the competition between chemical reaction and surface hops occurs in the same region of the potential energy surface.

(46) Ding, W. J.; Fang, W. H.; Liu, R. Z.; Fang, D. C. *J. Chem. Phys.* **2002**, *117*, 8745−8753.
(47) Yarkony, D. R. *J. Chem. Phys.* **2001**, *114*, 2601−2613.

Acknowledgment. All computations were carried out on an SP2 funded jointly by IBM (UK) and HEFCE (UK). L.B. is financed by the Ramón y Cajal program from the Spanish Ministerio de Ciencia y Tecnología (MCyT) and by Grant No. BQU2002-04112-C02-02 and BQU2002-03334 from the Dirección General de Investigación (MCyT).

Supporting Information Available: Semiclassical algorithm theory and implementation for CASSCF dynamics. Details for estimation of the energy gap at **TS**, second-order analysis at the CI (curvatures and energies of the states along the GD/IS coordinates, Table SI1), and details for construction of Figure 3 (Chart SI1). Summary of the trajectory results (Table SI2), discussion of a trajectory with an "extended mixed state" (Charts SI2−SI4), and details of the structural analysis (Tables SI3−SI7 and Chart SI5). This material is available free of charge via the Internet at http://pubs.acs.org.

JA043879H